Paper

Numerical Analysis of Wave Propagation Characteristics on a Buried Horizontal Conductor by an FDTD Method

Yoshihiro Baba* Member
Mohamed Nayel* Non-member
Naoto Nagaoka* Member
Akihiro Ametani* Member
Shozo Sekioka** Member

Fundamental characteristics of a 34-m long horizontal conductor buried at a depth of 1 m have been studied with an FDTD method. An equivalent radius of a buried thin wire is shown to be 0.23 times the side of cells employed, which is the same as that of an aerial thin wire. The rate of current dissipating from each section of the buried conductor to the injected current is roughly equal to that of the section length to the total length although it is somewhat influenced by the direction of a current lead. As the conductivity of the ground is higher, the wavefronts of a voltage and a current become less steep. The high permittivity distorts wavefronts of a voltage and a current with their propagation. However, its influence appears only initially and the response at the injection point is little influenced by it. The transient grounding resistance at 5 μs calculated by the FDTD method is 10 to 20% lower than the resistance calculated by Sunde's formula.

Keywords: FDTD method, grounding, transient, wave propagation

1. Introduction

The role of grounding electrodes is to dissipate fault currents effectively into the soil, and thereby to prevent damage of installations. Thus, the performance of power systems is influenced by proper functioning of grounding systems.

As no formulas of impedance and admittance have been derived even for a simple vertical or horizontal naked conductor buried in a homogeneous ground, transient characteristics of grounding electrodes have been investigated by experiments and recently by numerical electromagnetic analyses [(1)~(4)]. Generally in experiments, it has been difficult to know the conductivity and permittivity of the soil at a measurement site. Further, they might be inhomogeneous. This makes it difficult to understand the phenomena. On the other hand, a numerical electromagnetic analysis can be performed assuming a well-profiled condition that the values of these constants are known or set arbitrarily. Such a result is useful in understanding the phenomena as well as in confirming a measured result.

Among numerical electromagnetic analyses, those based on a finite-difference time-domain (FDTD) method [(5)] are quite effective to analyze the transient response of a grounding electrode. The accuracy of this method has been fully investigated in comparison with an experiment and shown to be satisfactory [(4)]. As this method requires long computation time and large capacity of memory, an analysis is restricted to a rather small space. A transient analysis of a large system or a system composed of various elements still need to be performed by such a tool as the Electro-Magnetic Transients Program (EMTP) [(6)]. One reasonable process of study, therefore, is to investigate the physical characteristics of a grounding electrode by a numerical electromagnetic analysis, and then to represent the obtained characteristics by a circuit model or to determine the values of its parameters.

In Ref. (7) and (8), wave propagation characteristics on a buried horizontal conductor have been studied by experiments. On the basis of the measured results, a circuit model, which regards the buried horizontal conductor as a uniform transmission line having shunt conductance, has been proposed [(7)]. Recently in Ref. (8), it has been indicated that a buried horizontal conductor might behave as a nonuniform transmission line. In the present paper, a transient response of a simple buried horizontal conductor is analyzed by the FDTD method. The main purpose of this paper is to clarify fundamental characteristics of a naked horizontal conductor buried in a homogeneous ground.

2. Method of Analysis

The FDTD method employs a simple way to discretize a differential form of Maxwell's equations. In the Cartesian coordinate system, it generally requires the entire space for an analysis to be divided into small rectangular

* Department of Electrical Engineering, Doshisha University
1-3, Miyakodani, Tatara, Kyotanabe 610-0321
** Kansai Tech Corp.
3-1-176, Fukuzaki, Minato-ku, Osaka 552-0013

cells and calculates the electric and magnetic fields of the cells using the discretized Maxwell's equations. As the material constants of each cell can be specified arbitrarily, a complex inhomogeneous medium can be easily analyzed. To analyze fields in an open space, an absorbing boundary condition has to be set on each plane which surrounds the space to be analyzed, so as not to produce reflections there. In the present analysis, the second-order Mur's method [9] is employed to represent absorbing planes. In Appendix 1, the validity of the authors' FDTD code is investigated in comparison with an experimental result [4] and shown to be satisfactory.

3. Models for Analysis

3.1 Buried Horizontal Conductor Figure 1(a) shows a side view of an analysis model. It simulates a naked horizontal conductor that is buried in a homogeneous ground and energized at its one end by a pulse voltage source. The length of the buried horizontal conductor is 34 m and its depth is 1 m. The voltage source produces a steep-front wave having a rise time of 10 ns, after which it maintains a magnitude of 1000 V. This voltage source is located at a height of 1 m over the ground and is connected with the buried horizontal conductor via a 1-m horizontal lead and a 2-m vertical lead. The other terminal of the source is connected with an overhead horizontal conductor of 9 m in length, which is in the same YZ-plane as the buried horizontal conductor is. The end of the overhead horizontal conductor is connected with a vertical electrode of 3 m in depth through a resistor. The value of this resistor is determined in section 4.1.

Figures 1(b) and (c) show the same model as Fig. 1(a) viewed from a different side and from above, respectively. A voltage reference line is set perpendicularly to the buried horizontal conductor and the current lead. The buried portion of the voltage reference line is insulated by a medium having the same relative permittivity as the ground does. There is a 0.25-m gap between the tip of the voltage reference line and the buried horizontal conductor. The voltage induced in this gap is defined as the voltage of the buried conductor in this paper. The horizontal part of the reference line is 30 m in length, and connected with a vertical lead that is buried up to a depth of 3 m. Also, a voltage is calculated by integrating electric fields from the horizontal conductor to an absorbing boundary. In this calculation, two integral paths as shown in Fig. 1(b) are chosen for comparison. One is a 37.5-m horizontal path at a depth of 1 m from the horizontal conductor to an absorbing boundary (Path I). The other is an 1-m vertical path from the horizontal conductor to the ground surface with a 37.5-m surface horizontal path from there to the absorbing boundary (Path II).

The conductivity of the homogenous ground σ is set to 5 mS/m and the relative permittivity ε_s is set to 12. The propagation velocity of an electromagnetic wave, v, in a lossy medium depends not only on permittivity but also on conductivity and frequency. Theoretically in this ground, for instance, v would be 86 m/μs at 100 MHz,

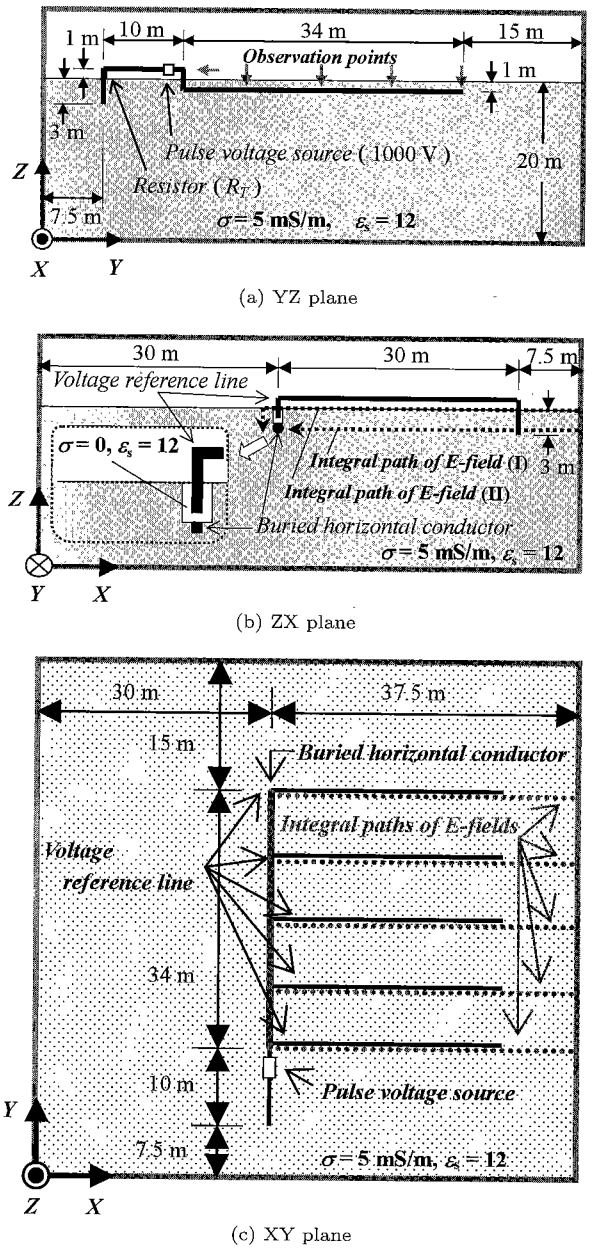

Fig. 1. An analysis model of a buried horizontal conductor energized at its one end by a pulse voltage source

81 m/μs at 10 MHz and 42 m/μs at 1 MHz. Note that the ionization of soil is not considered in this paper.

For the FDTD simulation, the conductor system shown in Fig. 1 is accommodated by a large rectangular analysis space of 67.5 × 66.5 × 28.5 m^3. The second-order Mur's absorbing condition is applied to all the planes surrounding the space to be analyzed. To model the system, cubic cells whose side is 0.25 m are used. In (10), the equivalent radius of a thin wire in air has been shown to be 0.23 Δs, where Δs is the side of the cubic cells employed. In Appendix 2 of the present paper, it is shown that an equivalent radius of a thin wire buried in a ground is also 0.23 Δs. As Δs is 0.25 m in the present analysis, the equivalent radius of thin wires in ground as well as in air is regarded as 57.5 mm.

The simulations are performed by a personal computer

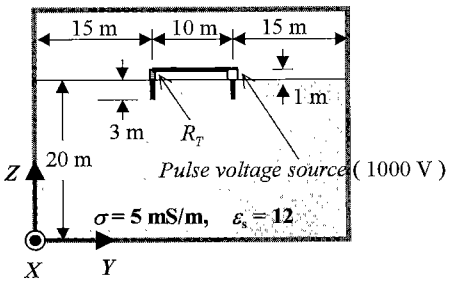

Fig. 2. An overhead horizontal conductor terminated by vertical grounding electrodes

with Pentium IV 1.7 GHz and 1024 MB RAM (about 500 MB of memory is needed in practice). Responses are calculated up to 5 μs with a time increment of 0.4 ns. The computation time for one case is about 30 hours.

3.2 Auxiliary Grounding of Current Lead

As the current lead in Fig. 1 is somewhat short, a matching resistor R_T is inserted between the current lead and the grounding vertical electrode to reduce successive reflections in the short current lead. To determine the value of the matching resistance, a simulation is carried out for a simple configuration as shown in Fig. 2 prior to the analysis of the horizontal electrode. The conductor system is accommodated by a rectangular analysis space of $30 \times 35 \times 28.5\,\mathrm{m}^3$. Each end of the overhead horizontal conductor is terminated by a vertical electrode buried up to 3 m. A voltage source is inserted between the vertical lead and the grounding electrode of the right-hand side. At the connection point of the left-hand side, a resistor is inserted.

4. Analyzed Results

4.1 Auxiliary Grounding of Current Lead

When the ground in Fig. 2 is perfectly conducting, a good matching condition is satisfied for the terminating resistance $R_T = 220\,\Omega$. Also from the initial ratio of the magnitude of the applied voltage V_A to that of the current I_S, almost the same value is obtained ($222\,\Omega = 1000\,\mathrm{V}/4.51\,\mathrm{A}$). Theoretically, the surge impedance of a horizontal conductor, of which height is 1 m and radius is 57.5 mm, is 213 Ω. The value, 220 or 222 Ω, estimated by the FDTD simulation is only 3 or 4% higher than this.

When the ground is finitely conducting, the characteristic impedance becomes dependent on frequency. Therefore, a matching condition cannot be fulfilled exactly by a constant resistor. However, a reasonable matching condition is realized when R_T is about 210 Ω in the FDTD simulation ($\sigma = 5\,\mathrm{mS/m}$).

In a steady state, I_S depends only on V_A, R_T and the grounding resistance of the vertical electrodes at both ends $2R_G$ ($I_S = V_A/(R_T + 2R_G)$). The value of I_S is 3.54 A, 3.42 A or 3.31 A for $R_T = 200\,\Omega$, 210 Ω or 220 Ω, respectively. Therefore, an identical value of $R_G = 41\,\Omega$ is obtained from each of these results. If the distance of these two electrodes is enlarged from 10 m to 20 m or 30 m, the increase of R_G is only 1 or 2 Ω, respectively. Note that R_G is little influenced even if the spacing

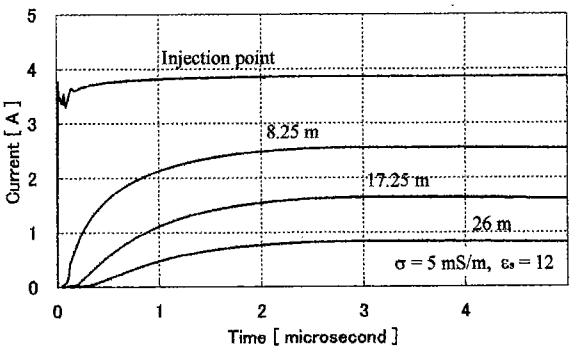

(a) Currents

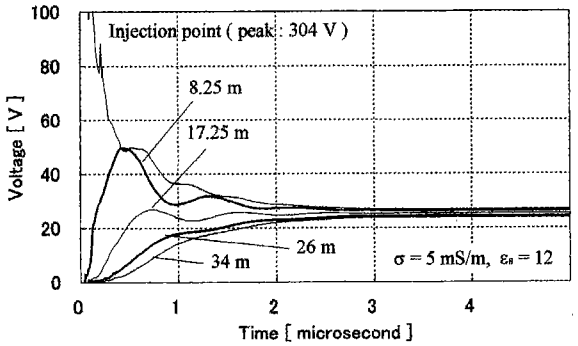

(b) Voltages evaluated by the voltage reference line

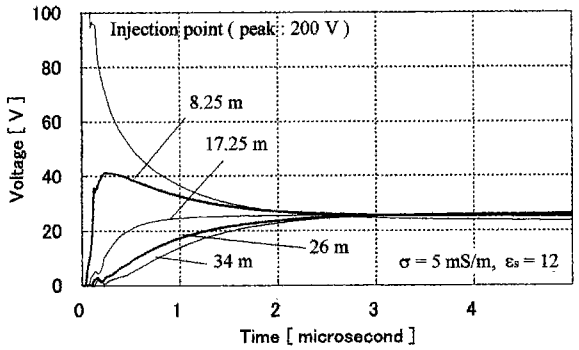

(c) Voltages evaluated by the electric-field integral

Fig. 3. Currents and Voltages at various points of the buried horizontal conductor in the case that $\sigma = 5\,\mathrm{mS/m}$ and $\varepsilon_s = 12$

between the electrode and the left or right absorbing boundary is shortened from 15 m to 7.5 m. Also, it is little influenced when the depth from the air-soil interface to the bottom absorbing boundary is reduced from 20 m to 10 m.

In consequence, the surge impedance of the current lead over the lossy ground is estimated to be about 250 Ω ($= R_T + R_G = 210\,\Omega + 41\,\Omega$). According to Deri's approximate expression [11], the characteristic impedance of the same conductor is about 240 Ω at 12.5 MHz ($= 300\,\mathrm{m}/\mu\mathrm{s}/(2 \times 12\,\mathrm{m})$; 12 m is the total length of the current lead). The value estimated by the FDTD simulation, 250 Ω, agrees well with this.

4.2 Buried Horizontal Conductor

Figure 3 shows currents and voltages at various points of the buried horizontal conductor in the case that σ is 5 mS/m and ε_s is 12. Figure 3(b) shows voltages evaluated by the voltage reference line, and Fig. 3(c) shows those

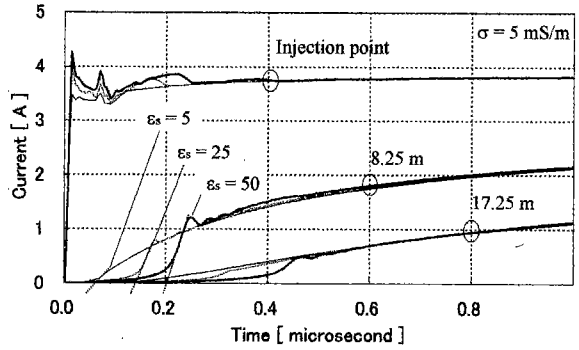

(a) Currents

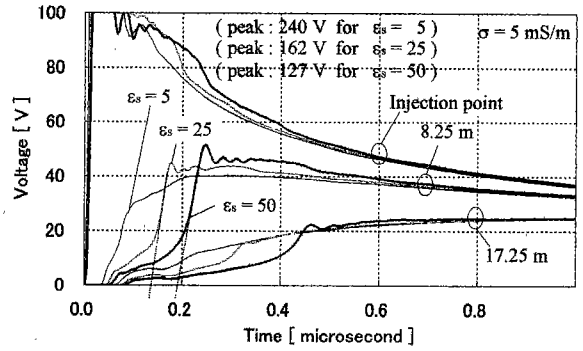

(b) Voltages evaluated by the electric-field integral

Fig. 4. Currents and Voltages of the buried horizontal conductor in the case that $\sigma = 5\,\mathrm{mS/m}$ and $\varepsilon_s = 5, 25$ or 50

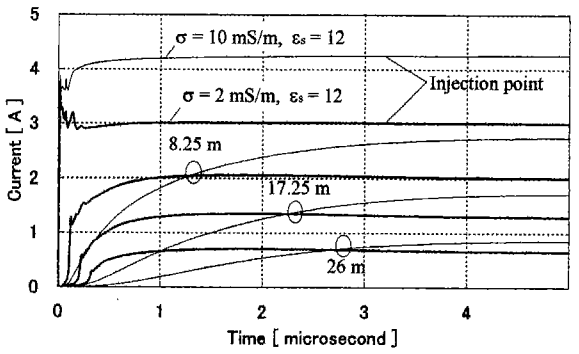

(a) Currents

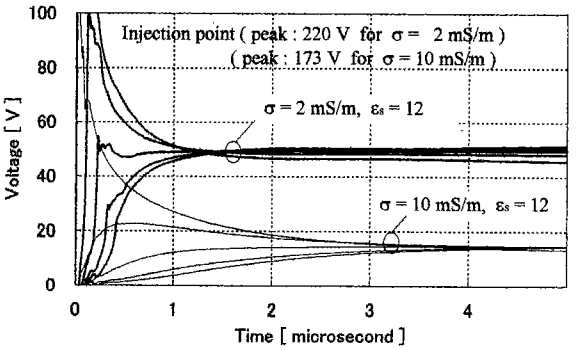

(b) Voltages evaluated by the electric-field integral

Fig. 5. Currents and Voltages of the buried horizontal conductor in the case that $\varepsilon_s = 12$ and $\sigma = 2$ or 10 mS/m

evaluated by the electric-field integral (Path I). Figure 4(a) shows currents in the case that σ is 5 mS/m and ε_s is 5, 25 or 50, and Fig. 4(b) shows voltages evaluated by the electric-field integral (Path I). Although only the initial 1-μs responses are shown in Fig. 4, the waveforms after this period are almost identical to that of Fig. 3 regardless of the relative permittivity. Figure 5 shows currents and voltages in the case that ε_s is 12 and σ is 2 or 10 mS/m. Figure 6 shows the responses for a 34-m insulated horizontal conductor buried at the same depth with those for the naked one. At the end of the insulated conductor, its core is connected with a 3-m naked horizontal electrode.

Note that the waveshapes of a voltage and a current are little influenced if the length of the current lead is enlarged from 10 m to 20 m. However, the transient-resistance value in the case for 20-m current lead becomes about 1 Ω higher than that for 10-m current lead (will be shown in section 5.4).

5. Discussion

5.1 Evaluation Methods of Voltages During the first 2 μs, voltages at the injection point, 8.25-m and 17.25-m points that are evaluated by an electric-field integral do not agree well with those evaluated by a voltage reference line as is found in Figs. 3(b) and (c). After that period, however, the waveforms evaluated by these two methods become similar. The initial rising portion evaluated by the electric-field integral is steeper than that evaluated by the other method, but the overshoot is smaller. The difference of voltages at 5 μs, evaluated by these two methods, is 2 to 10%. Note that there is little difference due to an integral path: an underground horizontal path (Path I) or a short vertical path to the ground surface with a horizontal path on the ground surface (Path II).

The waveforms of voltages evaluated by the voltage reference line are initially oscillatory. If the length of the voltage reference line is enlarged, the oscillation frequency becomes lower. Therefore, the initially oscillatory waveforms of voltages are probably associated with the successive reflections of an induced current in the voltage reference line. On the other hand, even if the integral path of electric fields is enlarged from 37.5 m to 47.5 m, the voltage waveform hardly changes.

5.2 Influence of Permittivity and Conductivity From Fig. 4, it is found that the wavefronts of current and voltage become concave with propagation along the buried horizontal conductor. After the initial rising period, however, each waveform becomes similar independent of permittivity. This is because the fast-front portion is much dissipated into the high-permittivity ground. The response at the injection point is little influenced by the permittivity of the ground except for the initial steep peak.

Table 1 shows the propagation velocity of a current wave evaluated by the travel time in the first 9.25 m (vertical 1 m and horizontal 8.25 m) from the injection point, and that of a voltage wave. The arrival time of a wave is defined as the intersection between the time axis and a straight line that is tangent to the wavefront at its steepest point. The times of arrival at 17.25 m,

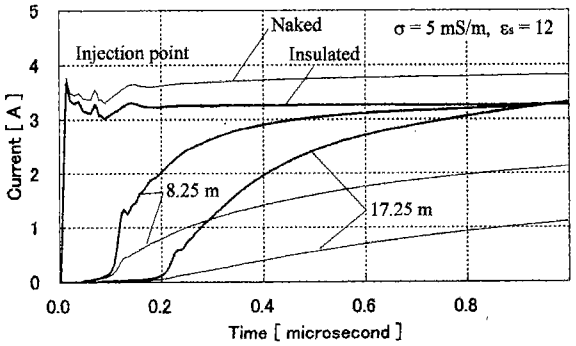

(a) Currents

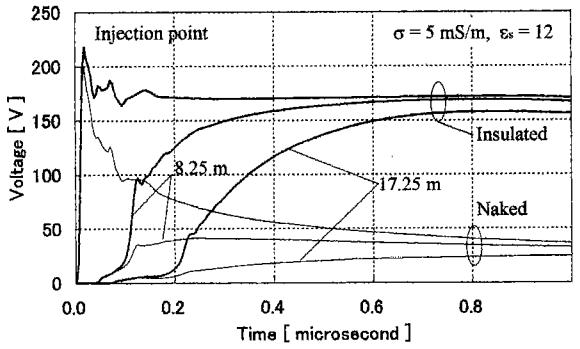

(b) Voltages evaluated by the electric-field integral

Fig. 6. Currents and Voltages of the buried naked horizontal conductor and those that the buried insulated conductor

Table 1. Propagation velocity of a current wave on the buried horizontal conductor and that of a voltage wave, evaluated by the travel time in the first 9.25 m section

	$\varepsilon_s = 5$	$\varepsilon_s = 25$	$\varepsilon_s = 50$
Current	134 m/μs	60 m/μs	42 m/μs
Voltage	168 m/μs	71 m/μs	49 m/μs

26 m and 34 m are not so obvious that the propagation velocity cannot be deduced reasonably from them. The apparent propagation velocity of a voltage wave deduced like this is faster than that of a current wave. This tendency has been found first in (8) by an experiment.

A current is a physical quantity that is based on the electric field at one point of interest ($\sigma \boldsymbol{E}$). On the other hand, a voltage is a physical quantity that is based on the sum or integral of a lot of electric-field elements ($\int \boldsymbol{E} \cdot d\boldsymbol{s}$). In the present analysis, the voltage of the buried horizontal conductor is evaluated as the sum of 150 electric-field elements ($150 \times 0.25\,\mathrm{m} = 37.5\,\mathrm{m}$) in the direction of X-axis ranging from the buried horizontal conductor to an absorbing boundary. In a lossy ground, high-frequency components of electric fields arrive early at each point along an electric-field integral path although the magnitude of each of these components is small. This is one of the reasons why the rise-time of the waveform of a voltage is shorter than that of a current. Note that on the surface of the ground electromagnetic waves propagate with the velocity of light. The initial gradual rise prior to the steep rise, which is obviously found in Fig. 4, is probably associated with the

Table 2. Rate of current dissipating from each section of the buried horizontal conductor to the total injected current (current lead is in parallel with the buried horizontal conductor)

σ [mS/m]	8.25 m + 1 m (26%)	9 m (26%)	8.75 m (25%)	8 m (23%)
2	34%	23%	21%	22%
5	34%	24%	21%	21%
10	35%	25%	20%	20%

* percentage in parenthesis is the rate of a section length to the total length.

electromagnetic waves penetrating into the ground from the surface. However, the initial gradual rise influences little on the arrival times and the velocities of a current wave and a voltage wave obtained on the basis of the definition stated above.

As the conductivity is higher, the wavefronts of voltage and current become less steep. The waveform of a voltage of the buried naked conductor is not similar to that of a current, particularly around the injection point. If the buried conductor is insulated, the waveform of a voltage is almost identical to that of a current just as it is a coaxial cable (Fig. 6).

5.3 Current Dissipation along Buried Horizontal Conductor Table 2 shows the rate of current dissipating from each section of the buried horizontal conductor to the total injected current evaluated at the moment of 5 μs of Figs. 3(a) and 5(a), at which electromagnetic field around the system is almost in a steady state. The rate of current dissipation is almost independent of the ground conductivity. However, the rate of current dissipating from the first 9.25-m section is somewhat higher than that from other part. Even if the 1-m vertical part of the buried conductor is insulated from the ground ($\sigma = 5\,\mathrm{mS/m}$ and $\varepsilon_s = 12$), this rate is hardly influenced: 32%, 25%, 21% or 22% dissipates from the first, second, third or fourth section, respectively. Even if the length of the current lead is enlarged from 10 m to 20 m, the ratio change little: 32%, 24%, 21% or 23%. When the current lead is stretched perpendicularly to the buried horizontal conductor, however, the rate of current dissipating from each section to the total injected current is almost equal to that of the physical length of each section to the total length. In this case, the rate of current dissipating from each section is 27%, 25%, 23% or 25%, respectively. As a consequence, it is shown that the current dissipates roughly uniformly from the buried horizontal conductor although the dissipation rate is somewhat influenced by the direction of a current lead or the location of grounding of the current lead.

5.4 Transient Grounding Resistance From Figs. 3 to 5, it is found that the responses almost settle down at around 5 μs. Table 3 shows the transient grounding resistance of the buried horizontal conductor that is calculated as the ratio of the voltage to the current at the injection point at 5 μs. The wavelength corresponding to the evaluation time is about 500 m, which is

Table 3. Transient grounding resistance evaluated at 5 μs from the waveforms calculated by the FDTD method and the steady-state resistance calculated by Sunde's formula

σ [mS/m]	FDTD	Sunde's formula	Difference
2	15.4 Ω	20.1 Ω	23%
5	6.2 Ω	8.1 Ω	23%
10	3.2 Ω	4.0 Ω	20%

about ten times longer than the length of the horizontal conductor. Hence, it is considered that the transient-resistance value at 5 μs is close to the resistance in the steady state. Sunde [12] has derived a theoretical formula of the DC resistance of a horizontal conductor buried in a homogeneous ground. It is expressed as follows:

$$R_{G.HOR} = \frac{1}{\pi\sigma l}\left[\ln\left(\frac{2l}{\sqrt{2rd}}\right) - 1\right].$$

where l is the length of the electrode, r is the radius and d is the depth of it. The values of transient grounding resistance obtained by the FDTD simulation for the arrangement of Fig. 1(a) are about 20% lower than those calculated by Sunde's formula regardless of the ground conductivity. When the length of the current lead is enlarged from 10 m to 20 m, 7.2 Ω is obtained from the FDTD calculation for σ being 5 mS/m. It is still 10% lower than that calculated by Sunde's formula. In the case that the 20-m long current lead is stretched perpendicularly to the buried horizontal conductor, 6.7 Ω is obtained. Therefore, it is clear that the transient grounding resistance is somewhat influenced by the length and the direction of a current lead.

Note that the voltages in the FDTD simulation are based on the integral of electric fields, of which path is 37.5 m in length. Even if it is enlarged to 47.5 m, the calculated voltage hardly changes. Hence, the lower resistance of the FDTD simulation compared with Sunde's formula is not ascribable to a finite length of electric-field integral.

Sunde has proposed a theoretical formula also for a vertical cylindrical electrode [12]. From this formula, 46 Ω is obtained for the vertical electrode shown in Figs. 1 and 2 (σ = 5 mS/m, d = 3 m and r = 57.5 mm). The values obtained by the FDTD analysis in section 4.1, which are 41 to 43 Ω, are about 10% lower than this. Sunde's formula gives 61 Ω for the vertical electrode studied in Appendix (σ = 2.28 mS/m, d = 3 m and r = 0.318 m) while an FDTD simulation gives 10% lower value (55 Ω). As this electrode is a rectangular prism having a cross section of 0.5 × 0.5 m^2, r is assumed to be the radius of an equivalent circle having the same circumference as the rectangular cross section has. As a consequence, Sunde's formula gives 10 or 20% higher value than the FDTD simulation does for a vertical or horizontal electrode, respectively. The conductivity of a ground is sometimes estimated by Sunde's formula from the measured grounding resistance. In such a case, somewhat higher conductivity might be estimated.

6. Conclusions

Fundamental characteristics of a naked horizontal conductor buried in a homogeneous ground have been studied by the FDTD method. An equivalent radius of a buried thin wire has been derived with the help of the concept proposed for an aerial thin wire. The waveform of a voltage of the buried naked conductor is not similar to that of a current. Further, the apparent propagation velocity of a voltage wave is faster than that of a current wave as was shown by an experiment [8]. A current is a physical quantity based on the electric field at a point of interest while a voltage of the buried horizontal conductor is evaluated as the sum or integral of a lot of electric-field elements. High-frequency components of electric fields arrive early at each point along an electric-field integral path for the evaluation of voltage although the magnitude of each of these components is small. This is probably one of the reasons why the rise-time of the waveform of a voltage is shorter than that of a current.

The rate of current dissipating from each section of the buried horizontal conductor to the total injected current is roughly equal to that of the section length to the total length although it is somewhat dependent on the direction of the current lead. As the conductivity is higher, the wavefronts of a voltage and a current become less steep. In inverse proportion to it, the resistance becomes small. The transient grounding resistance at 5 μs calculated by the FDTD method is 10 to 20% lower than the resistance calculated by Sunde's formula.

Acknowledgment

This work is supported by Japan Society for the Promotion of Science through Grant-in-Aid for Encouragement of Young Scientists (no.14750215).

(Manuscript received Feb. 28, 2003,
revised June 19, 2003)

References

(1) L. Grcev and F. Dawalibi: "An electromagnetic model for transients in grounding systems", *IEEE Trans. Power Delivery*, Vol.5, No.4, pp.1773–1781 (1990-10)

(2) S. Kato, T. Hirai, and S. Okabe: "Surge analysis of rod electrode for grounding by method of moment", 2002 National Convention Record, IEE Japan, no.7-168 (2002-3) (in Japanese)

(3) K. Tanabe: "Novel method for analyzing dynamic behavior of grounding systems based on the finite-difference time-domain method", *IEEE Power Engineering Review*, Vol.21, No.9, pp.55–57 (2001-9)

(4) K. Tanabe, A. Asakawa, T. Noda, M. Sakae, M. Wada, and H. Sugimoto: "Verifying the novel method for analyzing transient grounding resistance based on the FD-TD method through comparison with experimental results", CRIEPI Report, no.99043 (2000-5) (in Japanese)

(5) K.S. Yee: "Numerical solution of initial boundary value problems involving Maxwell's equation in isotropic media", *IEEE Trans. Antennas Propagation*, Vol.14, No.4, pp.302–307 (1966-5)

(6) W. Scott-Meyer: EMTP Rule Book, B.P.A (1977)

(7) S. Yamaguchi, M. Inoue, S. Sekioka, T. Sonoda, Y. Kato, N. Nagaoka, and A. Ametani: "A frequency-dependent counterpoise model for a transient analysis", Proc. ICEE'98,

pp.753–756, Kyongju, Korea (1998-7)
(8) A. Ametani, M. Nayel, S. Sekioka, and T. Sonoda: "Basic Investigation of wave propagation characteristics on an underground naked conductor", Proc. ICEE 2002, pp.2141–2146, Jeju, Korea (2002-7)
(9) G. Mur: "Absorbing boundary conditions for the finite-difference approximation of the time-domain electromagnetic-field equation", *IEEE Trans. Electromagnetic Compatibility*, Vol.23, No.4, pp.377–382 (1981-11)
(10) T. Noda and S. Yokoyama: "Thin wire representation in finite difference time domain surge simulation", *IEEE Trans. Power Delivery*, Vol.17, No.3, pp.840–847 (2002-7)
(11) A. Ametani: Distributed-Parameter Circuit Theory, Corona Pub. Co., Tokyo (1990) (in Japanese)
(12) E.D. Sunde: Earth Conduction Effects in Transmission Systems, Dover, New York (1968)

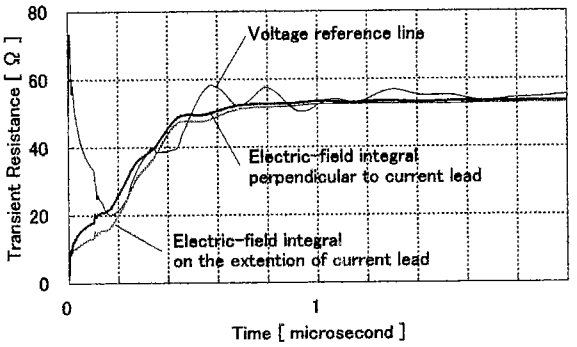

app. Fig. 1. Transient grounding resistance of a 3-m vertical electrode calculated by the authors' FDTD code

Appendix

1. Accuracy of the FDTD Simulation

In (4), an experiment of transient grounding resistance has been carried out to investigate the accuracy of their FDTD code. In the experiment, a simple conductor system comprising a vertical grounding electrode, a current lead and a voltage reference line was employed. The radii of the electrode and the current lead were sufficiently large so that the system should be modeled reasonably by the FDTD method.

The cross section of the vertical grounding electrode was $0.5 \times 0.5\,\mathrm{m}^2$ and the length was 3 m. A current lead was 20 m in length and 67.5 mm in radius. It was stretched horizontally at a height of 1 m, and was connected with the grounding electrode via a damping resistor of 800 Ω and a pulse voltage generator. The magnitude of a produced voltage was about 500 V and the nominal risetime was 63 ns. An injected current was measured at this point with a current transformer. The other end of the current lead was grounded through a vertical lead, which was buried up to a depth of 1.5 m. A voltage reference line was 50 m in length and 0.8 mm in radius. It was stretched horizontally at a height of 1.5 m and perpendicularly to the current lead. It was stretched down at its close end to the grounding electrode. There, a voltage between the electrode and the voltage reference line was measured with a voltage probe. At the other end, it was stretched down and connected with a cylindrical electrode of 0.125 m in radius and 1.5 m in depth.

The relative permittivity of the soil at the measurement site was estimated to be about 50 from a radar measurement. The conductivity was estimated to be from 1.91 to 3.23 mS/m on the basis of measured steady-state grounding resistance. In the calculation, therefore, 2.28 mS/m was assumed.

In an FDTD simulation (4), the above conductor system was represented with cubic cells of $0.25 \times 0.25 \times 0.25\,\mathrm{m}^3$. It was accommodated by a rectangular analysis space of $80 \times 50 \times 50\,\mathrm{m}^3$. The second-order Liao's absorbing condition was applied to all the planes of this rectangular space. The waveforms of a calculated transient voltage and current were shown to be in fairly good agreement with those of measurement (4).

In the present paper, a similar calculation is carried out to investigate the accuracy of the authors' FDTD code. In the code, the second-order Mur's absorbing condition is employed.

app.Fig. 1 shows the time variation of the transient grounding resistance deduced as the instantaneous ratio of the voltage of the electrode to the injected current. The transient voltages are calculated by three ways. One is the gap voltage induced between the top of the 3-m vertical electrode and the voltage reference line. The other two are the voltages obtained by integrating electric fields on the surface of the ground from the top of the electrode to an absorbing boundary. One integral path is perpendicular to the current lead, and the other is on the extension of the current lead. The integral path is 25 m in both cases. Although the transient voltage or resistance based on the electric-field integral is initially influenced by the direction of integral path, it settles down to an identical value after 1 μs or so regardless of integral path. The resistance evaluated by the voltage reference line is not so much different from that evaluated by field integral although it includes some oscillation. The calculated waveform in the case using the voltage reference line agrees well with the measured waveform (4). The settling value of the transient grounding resistance is about 55 Ω regardless of evaluation method, and it agrees well with the measured value (4).

2. Derivation of an Equivalent Radius of a Buried Thin Wire

In (10), it has been shown that an aerial thin wire has some equivalent radius in the case that the electric-field elements along the thin wire are forced to be zero. When the side of cubic cells employed is Δs, the equivalent radius is $0.23\,\Delta$s. In the present paper, an equivalent radius of a naked thin wire buried in a ground is derived with the help of the concept proposed in Ref. (10).

app.Fig. 2 illustrates the cross section of a thin wire surrounded by a cylindrical sheath conductor. The radii of the thin wire and the sheath are a and b, respectively. The conductivity and the relative permittivity of a medium between the thin wire and the sheath conductor are σ and ε_s, respectivily. In this condition, the conductance between the thin wire and the sheath is $2\pi\sigma/\ln(b/a)$ and the susceptance is $2\pi\varepsilon_0\varepsilon_s\omega/\ln(b/a)$. Therefore, the conductance becomes

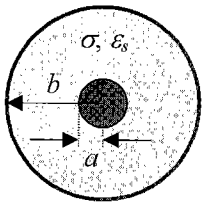

app. Fig. 2. Cross section of a thin wire surrounded by a cylindrical sheath

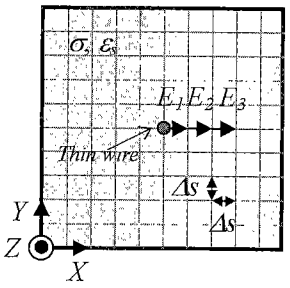

app. Fig. 3. Electric fields around a thin wire in a rectangular sheath to be used for an FDTD simulation

equal to the susceptance when the frequency is

$$f = \sigma/(2\pi\varepsilon_0\varepsilon_s).$$

For a medium of $\sigma = 5\,\mathrm{mS/m}$ and $\varepsilon_s = 12$, f is 7.5 MHz. If the frequency is lower than this, the conductance becomes dominant and the conduction current in a radial direction is larger than the displacement current. Therefore, electric fields in the medium are mainly determined by σ after several hundreds nanoseconds.

app.Fig. 3 shows the cross section of a thin wire surrounded by a rectangular sheath conductor for an FDTD simulation. The cross-sectional area of the sheath is 2.5 $\times$ 2.5 m^2 and the length is 25 m. This conductor system is represented with cubic cells whose side is 0.25 m. A voltage, which has a rise time of 20 ns and a magnitude of 100 V, is applied between the thin wire and the sheath at its one end. The other end is open. A time increment is set to 0.4 ns for this simulation.

app.Fig. 4 shows the time-variations of the ratios of E_1, E_2 and E_3 to E_2 in app.Fig. 3, which are radial electric fields calculated at 12.5 m from the ends of the conductor. It is found that the ratios settle down after 100 ns or so and they are almost equal to those calculated for a thin wire in air [10]: 2.21, 1.00 and 0.59. This is natural because both the conductance and the susceptance of a thin wire follow similar expressions as were shown above. Also, the ratios change little even if a different conductivity 25 or 50 mS/m is employed and a different time increment 0.25 or 0.48 ns is used. Thus, the electric field around the thin wire can also be approximated by the following function [10]:

$$E = 3\Delta s/(2x).$$

This is normalized so that E_2 should be unity. app.Fig. 5 shows the radial electric fields calculated by this function and those obtained by the FDTD simulation.

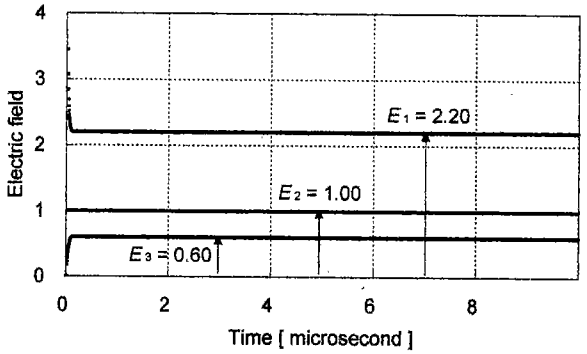

app. Fig. 4. Time-variations of the ratios of E_1, E_2 and E_3 to E_2 calculated by the FDTD method in the case of $\sigma = 5\,\mathrm{mS/m}$ and $\varepsilon_s = 12$

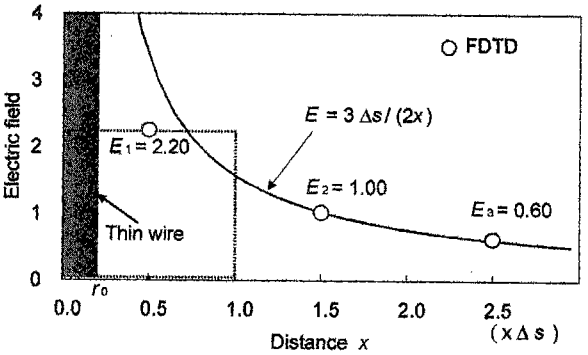

app. Fig. 5. Radial electric fields around the thin wire

If the equivalent radius of the thin wire now in question is assumed to r_0 and the electric field is assumed to follow the above function, the potential difference between $x = 0$ and $x = \Delta s$ is given as follows:

$$\int_{r_0}^{\Delta s} E\,dx = \frac{3\Delta s}{2}\ln\frac{\Delta s}{r_0}.$$

If the above expression is equated to 2.2 Δs, which is the potential difference obtained by the FDTD simulation, the equivalent radius is given as

$$r_0 = 0.23\Delta s.$$

This is the equivalent radius of a naked thin wire buried in a ground.

Yoshihiro Baba (Member) was born in Wakayama, Japan, on February 24, 1971. He received B.Sc., M.Sc. and Dr.Eng. degrees from the University of Tokyo in 1994, 1996 and 1999, respectively. He joined the Faculty of Engineering, Doshisha University in 1999. He is currently a Lecturer there. Dr. Baba is a member of both IEE and IEEE.

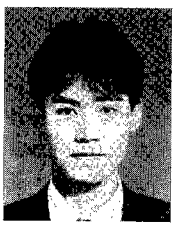

Mohamed Nayel (Non-member) was born in Assiut, Egypt, on April 15, 1973. He received B.Sc. and M.Sc. degrees from Assiut University, Assiut, Egypt, in 1996 and 1999, respectively. He was employed by Assiut University in 1996 and became an Assistant Lecturer in 1999. He has been a Ph.D. student in Doshish University, Japan, since 2000.

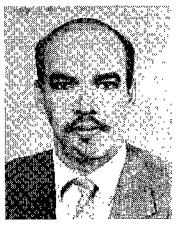

Naoto Nagaoka (Member) was born in Nagoya, Japan, on October 21, 1957. He received B.Sc., M.Sc. and Dr.Eng. degrees all from Doshisha University in 1980, 1982 and 1993, respectively. He joined the Faculty of Engineering, Doshisha University in 1985, and has been a Professor since 1999. Dr. Nagaoka is a member of both IEE and IEEE.

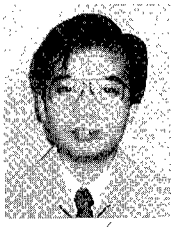

Akihiro Ametani (Member) was born in Nagasaki, Japan, on February 14, 1944. He received B.Sc. and M.Sc. degrees from Doshisha University in 1966 and 1968, respectively, and Ph.D. degree from the University of Manchester in 1973. He had been with Doshisha University from 1968 to 1971, the University of Manchester Institute of Science and Technology from 1971 to 1974, and Bonneville Power Administration for summers from 1976 to 1981. He became a Professor at Doshisha University in 1985. He had been the Director of the Institute of Science and Engineering from 1997 to 1998, and the Dean of Library and Computer/Information Center in the same university from 1998 to 2001. Dr. Ametani is a Chartered Engineer in the U.K., a Distinguished Member of CIGRE and a Fellow of both IEE and IEEE.

Shozo Sekioka (Member) was was born in Osaka, Japan, on December 30, 1963. He received B.Sc. and Dr.Eng. degrees from Doshisha University in 1986 and 1997, respectively. He joined Kansai Tech Corporation in 1987, and has been engaged in the lightning surge analysis in electric power systems. He is a member of IEE, and Society of Atmospheric Electricity of Japan.